Supplement of Geosci. Model Dev., 13, 1663–1683, 2020
https://doi.org/10.5194/gmd-13-1663-2020-supplement

Geoscientific Model Development
Open Access
EGU

Supplement of

Lower boundary conditions in land surface models – effects on the permafrost and the carbon pools: a case study with CLM4.5

Ignacio Hermoso de Mendoza et al.

Correspondence to: Hugo Beltrami (hugo@stfx.ca)

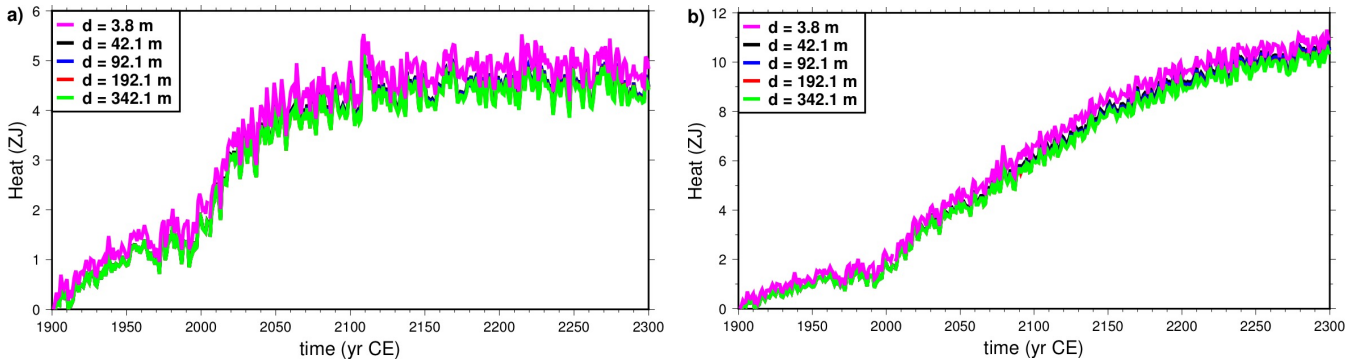

Figure S1. Heat stored in the soil (upper 3.8 m), for models of subsurface thickness d of 3.8 m (magenta), 42.1 m (black), 92.1 m (blue) 192.1 m (red), and 342.1 m (green). a) Simulations forced with CRUNCEP + RCP 4.5 data. b) Simulations forced with CRUNCEP + RCP 8.5 data. Note the vertical scale difference between the two panels.

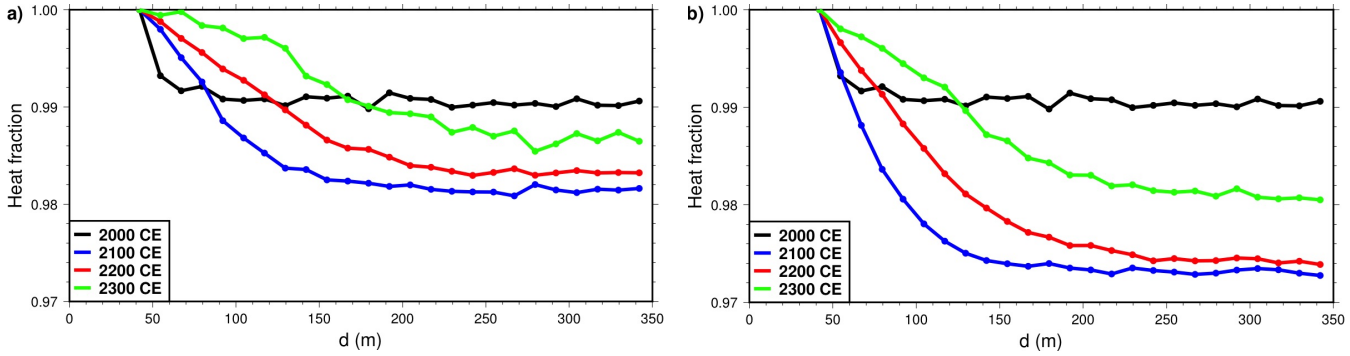

Figure S2. Heat stored in the soil as function of subsurface thickness, as fraction of that the original model ($d = 42.1$ m). Years 2000 (black), 2100 (blue), 2200 (red) and 2300 (green). a) Simulations forced with CRUNCEP + RCP 4.5 data. b) Simulations forced with CRUNCEP + RCP 8.5 data. Note the vertical scale difference between the two panels.

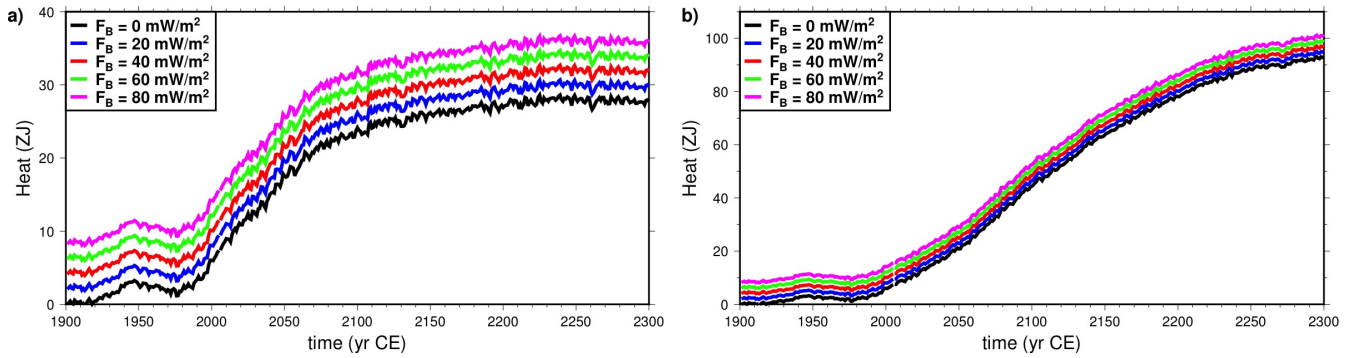

Figure S3. Heat stored in the upper 42.1 m (the thickness of all models is 42.1 m) as function of crustal heat flux, relative to the initial heat content of the original model ($F_B = 0$ mW m^{-2}). The heat content in each model is a static shift from that of the original model. a) Simulations forced with CRUNCEP + RCP 4.5 data. b) Simulations forced with CRUNCEP + RCP 8.5 data. Note the vertical scale difference between the two panels.

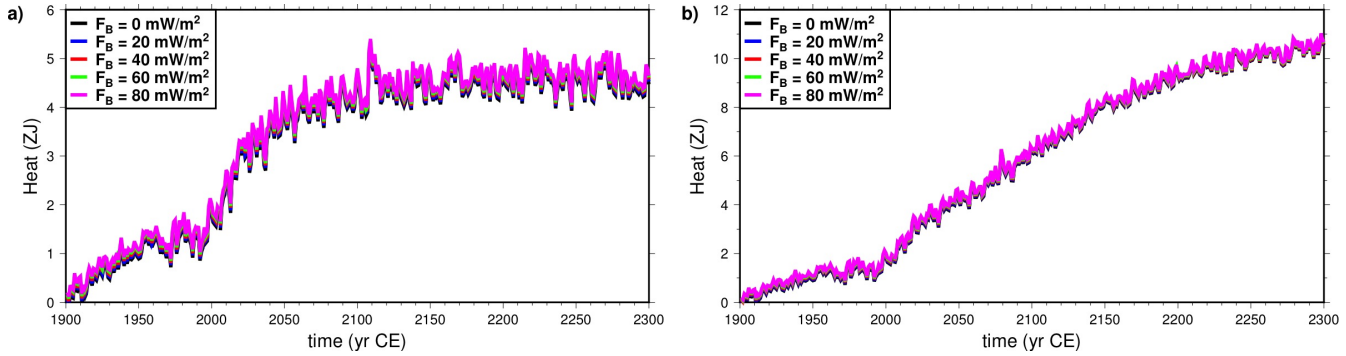

Figure S4. Heat stored in the soil (upper 3.8 m) as function of crustal heat flux, relative to the initial heat content of the original model ($F_B = 0$ mW m^{-2}). a) Simulations forced with CRUNCEP + RCP 4.5 data. b) Simulations forced with CRUNCEP + RCP 8.5 data. Note the vertical scale difference between the two panels.

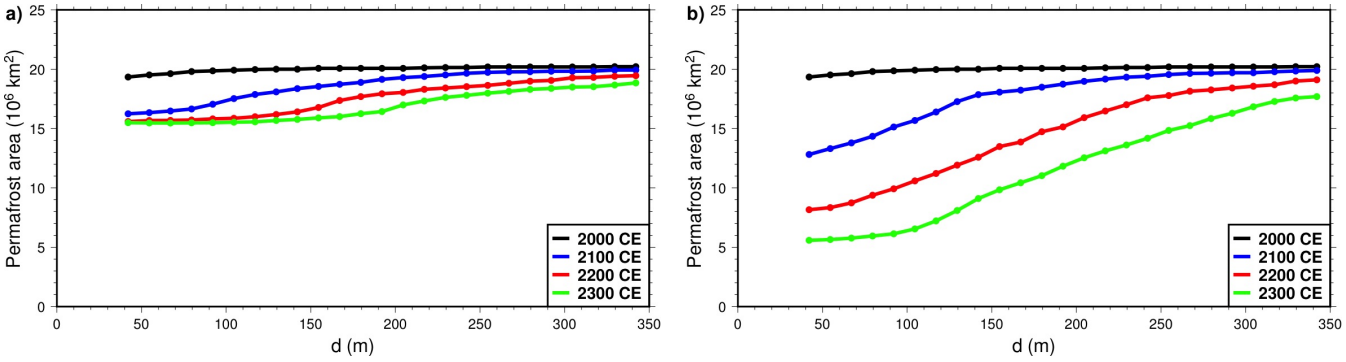

Figure S5. Northern Hemisphere intermediate-depth permafrost area as function of subsurface thickness d, at the years 2000 (black), 2100 (blue), 2200 (red) and 2300 (green). a) Simulations forced with CRUNCEP + RCP 4.5 data. b) Simulations forced with CRUNCEP + RCP 8.5 data.

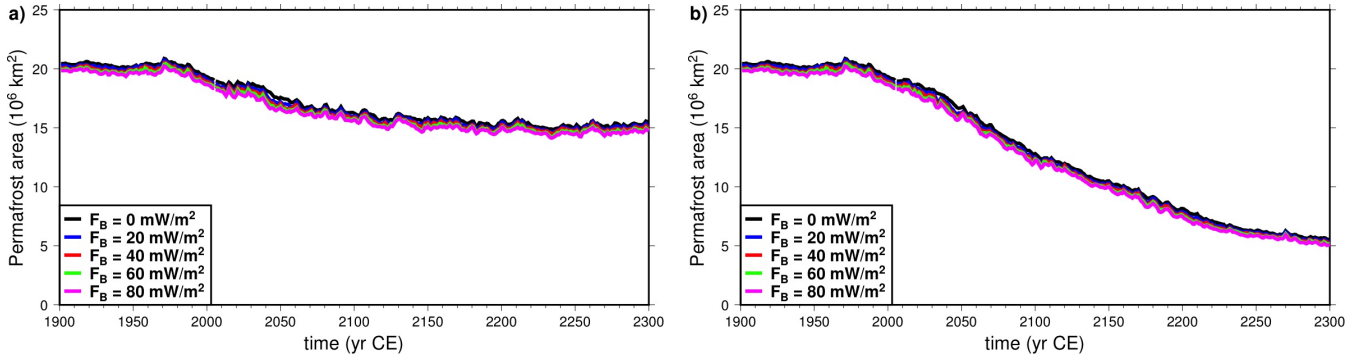

Figure S6. Northern Hemisphere intermediate-depth permafrost area as function of time. Model versions using different heat flux as bottom boundary. a) Simulations forced with CRUNCEP + RCP 4.5 data. b) Simulations forced with CRUNCEP + RCP 8.5 data.

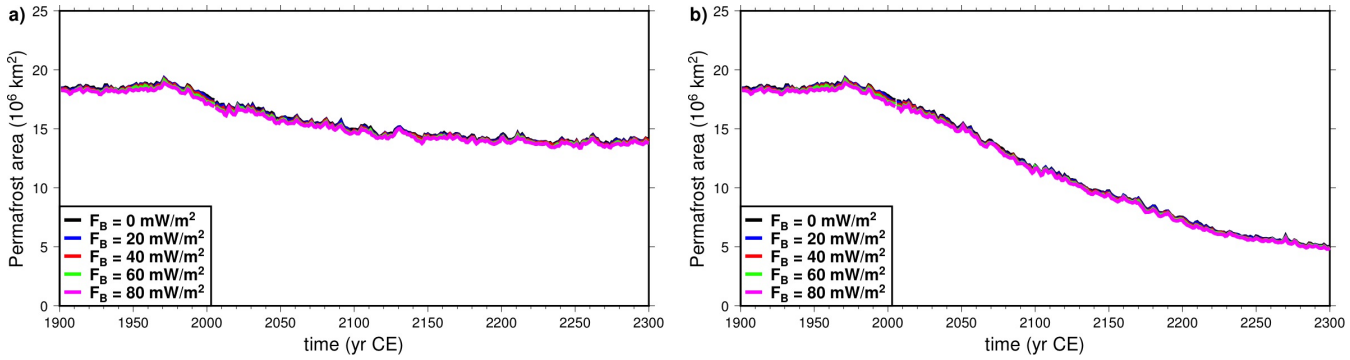

Figure S7. Northern Hemisphere near-surface permafrost area as function of time. Models using different heat flux as bottom boundary. a) Simulations forced with CRUNCEP + RCP 4.5 data. b) Simulations forced with CRUNCEP + RCP 8.5 data.

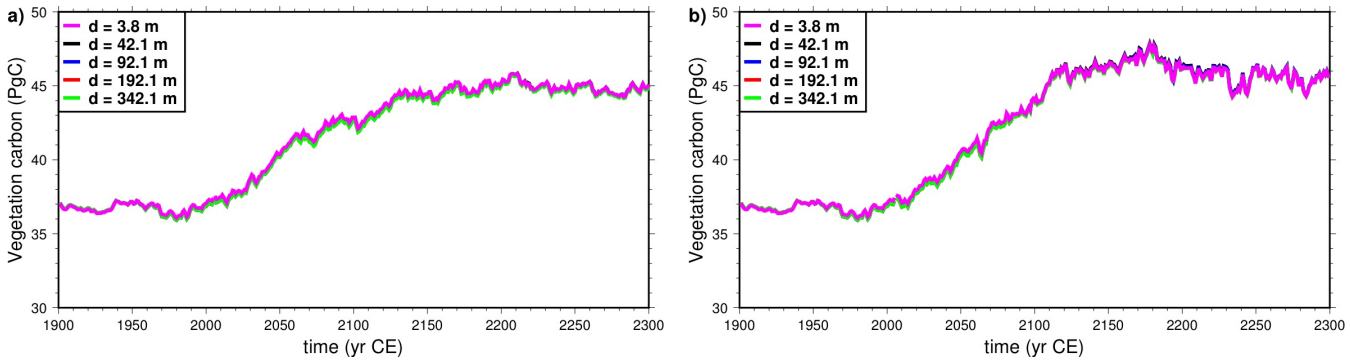

Figure S8. Vegetation carbon pool in the Northern Hemisphere permafrost region. Models with varying bottom boundary depth. a) Simulations forced with CRUNCEP + RCP 4.5 data. b) Simulations forced with CRUNCEP + RCP 8.5 data.

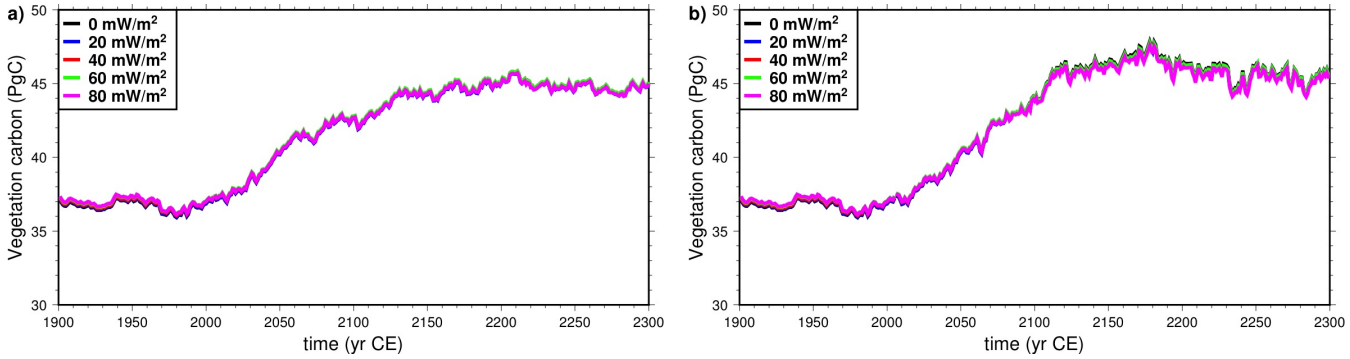

Figure S9. Vegetation carbon pool in the Northern Hemisphere permafrost region. Models with varying basal heat flux. a) Simulations forced with CRUNCEP + RCP 4.5 data. b) Simulations forced with CRUNCEP + RCP 8.5 data.

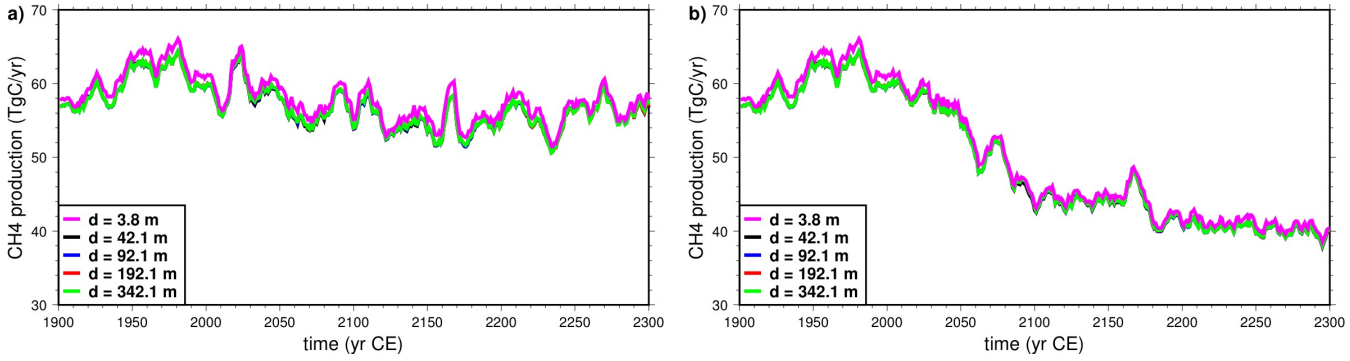

Figure S10. Global yearly methane production as function of time, moving average of 10 years. Models with varying bottom boundary depth. a) Simulations forced with CRUNCEP + RCP 4.5 data. b) Simulations forced with CRUNCEP + RCP 8.5 data.

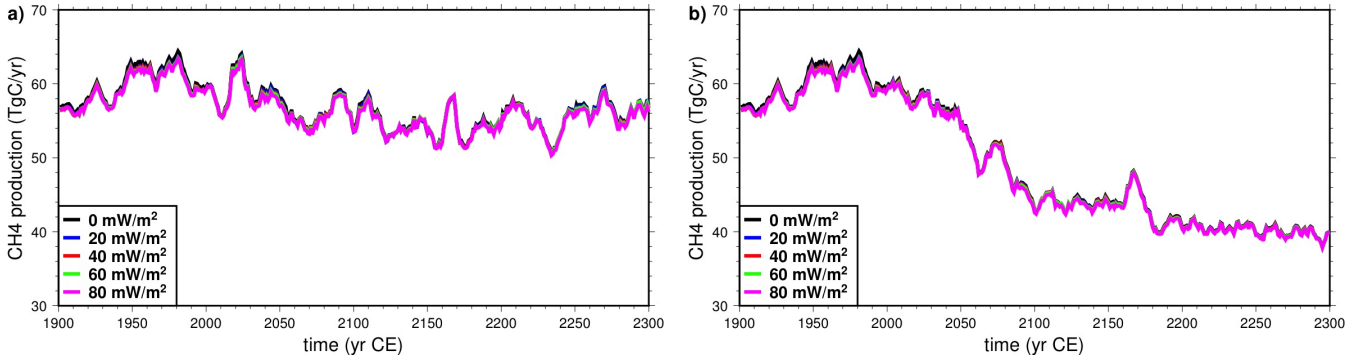

Figure S11. Global yearly methane production as function of time, moving average of 10 years. Models with varying basal heat flux. a) Simulations forced with CRUNCEP + RCP 4.5 data. b) Simulations forced with CRUNCEP + RCP 8.5 data.